

1 CSO Reduction through a Safe Real-Time Control based on Multi-Reinforcement
2 Learning, system optimization, and Model Predictive Control

3 Zhenliang Liao^{1,2,3,4,5}, Wenchong Tian^{2,3†}, Guozheng Zhi⁶, Xuan Wang^{2,3}.

4 ¹ College of Civil Engineering and Architecture, Xinjiang University, 830046, Urumqi,
5 China.

6 ² State Key Laboratory of Pollution Control and Resource reuse, College of
7 Environmental Science and Engineering, Tongji University, 200092 Shanghai, China.

8 ³ Key Laboratory of Yangtze River Water Environment, Ministry of Education, Tongji
9 University, 200092 Shanghai, China.

10 ⁴ Shanghai Institute of Pollution Control and Ecological Security, Shanghai 200092,
11 P.R. China.

12 ⁵ UNEP-Tongji Institute of Environment for Sustainable Development, College of
13 Environmental Science and Engineering, Tongji University, Shanghai 200092, China.

14 †Corresponding author: Wenchong Tian

15 ⁶ Shanghai Urban Water Resources Development and Utilization National Engineering
16 Center Co. L td., Shanghai 200082, China

17
18 Email address: wenchong@tongji.edu.cn

19 Tel: +86 18817870656
20

21 Abstract

22 Real-time control (RTC) helps the combined sewer system to adapt its response
23 to individual rainfall and enhance the performance of combined sewer overflow (CSO)
24 reduction. Recently, an RTC approach based on reinforcement learning (RL) is
25 developed for flooding control in a stormwater system. However, the safety and the
26 performance of this AI algorithm still need further improvement. In this paper, a new
27 RTC method based on multiple RLs, system optimization, and model predictive
28 control (MPC) is developed for the improvement of both safety and CSO reduction.
29 First, five RL agents are trained by five individual RL algorithms. Then, an
30 optimization model is used to optimize the advantage function of all the agents for
31 control effect improvement. After that, an MPC-based security system is established
32 to check the safety of control strategy before the implementation. Finally, our new
33 RTC model, called voting system, is developed through the combination of these five
34 agents and the security system. This method is evaluated in the combined sewer
35 system model of a city in eastern China. According to the results: (i) All the five
36 trained RLs are able to show promise in overflow reduction. (ii) The AFI improves
37 the CSO reduction of all the agents with the maximum improvement rate of 44.5%.
38 (iii) The security system selects a safe control strategy through a small scale MPC,
39 thus it provides a guarantee of safety. Still, our method faces the challenges of
40 computing time, local optimization, and the limitation of system capacity.

41

42 **Key words:** safety, reinforcement learning, combined sewer system, real-time control,
43 model predictive control, combined sewer overflow.

44

45 1. Introduction

46 The combined sewer system is widely used in many cities around the world.
47 However, the combined sewer overflow (CSO) cannot be easily avoided during
48 application (Mailhot et al., 2015; Suarez and Puertas, 2005; Wan and Lemmon, 2007;
49 Xu and Liao, 2013; Xie et al., 2017; Gu et al., 2017). A primary solution to this
50 problem is to enhance the infrastructure for optimized system-scale performance. But
51 the cost and viability of this solution is highly variable in different cases (Abhiram et
52 al., 2020).

53 Another solution is real-time control (RTC), which uses sensor data to infer the
54 real-time state of a combined sewer system and responds via control of distributed
55 control assets, such as valves, gates, and pumps (Rauch and Harremoes, 1999. Kerkez
56 et al., 2016; Lund et al., 2018; Lund et al., 2020). By achieving system-level
57 coordination between many distributed control elements, only a small set of
58 infrastructures are needed to optimize system operation for lower overflow and
59 flooding (Schütze et al., 2002; Kerkez et al., 2016).

60 Recently, some researchers provided a new type of RTC methods based on
61 reinforcement learning (RL) and proved that it is capable of control a stormwater
62 system in real-time for flow control and flooding reduction (Ochoa et al., 2019;
63 Abhiram et al., 2020). However, challenged by the risk of handing over the control
64 process to a computer, it presently shows that an independent security system is
65 strongly demanded to guarantee the safety of the RL method in real-world operation.
66 Meanwhile, it is still necessary to further improve the control effect of the RL method
67 in the combined sewer system.

68 Considering the improvement of both the safety and the control effect of the
69 existing RL system, a new RTC method based on multi-RL, system optimization, and
70 model predictive control (MPC) is developed in this study. First, five RL algorithms
71 are used to train five individual agents. Then an optimization model of combined
72 sewer system is employed to optimize the advantage function of these RL agents, thus
73 further improves their control effect. After that, an independent security system,
74 which is based on a small scale MPC, is established to check the safety of control
75 strategy before implementing it. Finally, our new RTC method, called voting system,
76 is established through the combination of these five RL agents and the security system.
77 Accordingly, the contributions of this paper include: 1. Using multiple RL methods,
78 including both value-based and policy-based, to illustrate the effectiveness of
79 different RL models on CSO reduction; 2. Improving the control effect of RL models
80 through an optimization model based on the combined sewer system; 3. Designing an
81 independent security system based on MPC to provide a guarantee of safety.

82 The remainder of this paper is organized as follows: In Section 2, we briefly
83 introduce some related works, including the RTC in the urban drainage systems, the
84 RL, and the concept of safe RL. In Section 3, we describe the details of our method.
85 The case study is introduced in Section 4. And the use of our method in the case study

86 is given in Section 5. For comparison, the use of other RL methods is also provided.
87 Considering the risk to property and public safety, the evaluation of these methods is
88 established across a series of simulations, which span various rainfall events with a
89 mathematical model (SWMM). In Section 6, the effect of CSO reduction, the safety
90 of the voting system, and some remaining challenges are discussed. Finally, our
91 conclusions are shown in Section 7.

92 2. Preliminaries and related works

93 2.1. RTC of urban drainage system and model predictive control

94 A combined sewer system is controlled in real time if process variables are
95 monitored and used to operate actuators of the system (Schütze et al., 2002). In a
96 control loop of an RTC system, the sensors monitor process variables and send it to
97 controllers. The controllers operate actuators according to control strategy. Then, the
98 actuators influence the process to optimize system operation (Schütze, et al., 2002).

99 A control strategy or “control procedure” is defined as the time sequence of
100 set-points given by controller (Schütze, et al., 2002). To generate the control strategy,
101 one of the efficient ways is the model predictive control (MPC, Fig.1), which
102 recursively repeats the optimization of the control strategy based on a rainfall
103 prediction within a finite time horizon and move forward according to the receding
104 horizon principle (Fu et al., 2008; Joseph et al., 2015; Lund et al., 2018). Although
105 MPC faces the problems of high computation load and uncertainty prediction, it is
106 still widely used in many cases (Sebastian and Stefan, 2019; Lund et al., 2020;
107 Congcong et al., 2020).

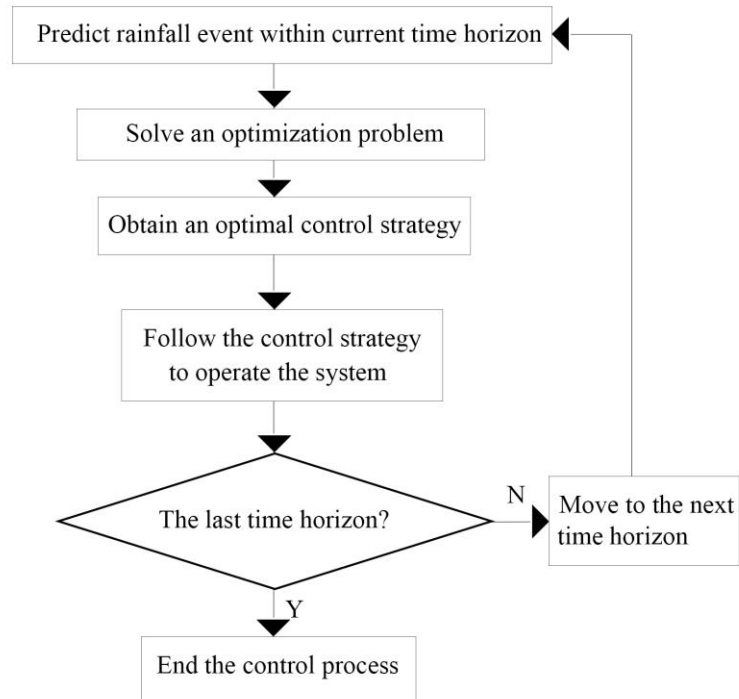


Fig.1. The schematic MPC

108

109

110 2.2. Multi-reinforcement learning

111 2.2.1. Brief review of reinforcement learning

112 Reinforcement learning (RL) is a kind of model used for control and planning
 113 (Sutton and Barto, 2018). The goal of RL is to learn an optimal control strategy from
 114 experimental trials and relatively simple feedback. For now, the RL has emerged as a
 115 state-of-the-art methodology for many autonomous control systems, such as
 116 autonomous driving (Pan et al., 2017), stock trading (Tan et al., 2011), AI gaming
 117 (Wu et al., 2018; Shao et al., 2018; Silver et al., 2017), reservoir scheduling systems
 118 (Madani and Hooshyar, 2014, Castelletti et al., 2013), flow control (Ochoa et al.,
 119 2019), in-line storage control (Labadie, 2014) and watershed flooding control
 120 (Abhiram et al.,2020).

121 Usually, an RL model includes an agent with a behavior function (policy) and an
 122 environment that is controlled by the agent. The environment provides state (s_t) of
 123 current time point t , and the agent choose to take an action (a_t) of next time step
 124 according to the given state and its policy. Once an action is taken, the environment
 125 delivers a reward (r_t) as feedback. With the help from the state, action, reward, the
 126 agent is able to master the control process and adapt to the environment actively to
 127 maximize expected future rewards (called value function, or Q value).

128 2.2.2. Multi-RL methods

129 Many RL models have been developed in recent years, including deep Q learning
130 and dueling deep Q learning (Minh et al., 2015), proximal policy optimization
131 (Schulman et al., 2017), and advance Actor-Critic (Sutton et al., 1999; Minh et al.,
132 2016). These methods are classified as policy-based and value-based.

133 (1) Deep Q learning and dueling deep Q learning

134 Deep Q neural network learning (DQN) and dueling deep Q neural network
135 learning (DDQN) are two methods belonging to value-based family. DQN is based on
136 the theory of Q learning, but take advantage from deep neural network to maximum
137 the Q value (Eq. (1), where a_t , s_t , r_t are action, state, and reward according to
138 above, θ is the parameters of neural network, γ is a hyperparameter called the
139 discount factor), to find the parameters enlarging the total expected reward during
140 control process (Minh et al., 2015; Sutton and Barto, 2018).

$$140 \quad q(a_t, s_t, \theta) = \mathbb{E}_t \left[\sum_{k=0}^{\infty} [\gamma^k r_{t+k+1} | a_t, s_t, \theta] \right] \quad (1)$$

141 DDQN uses two deep neural networks to approximate the optimal Q value (Van
142 2010), one of them is to determine the optimal policy and the other is to determine the
143 Q value (Van et al., 2016; Wang et al., 2016). In this way, DDQN avoids
144 overoptimistic value estimates problem of DQN.

145 (2) Proximal policy optimization

146 Proximal policy optimization models, including PPO1 and PPO2, are the
147 policy-based reinforcement learning models (Schulman et al., 2015; Schulman et al.,
148 2017). PPO1 tries to find the best policy function (input state, and output action) by
149 computing an estimator of the policy gradient (Eq. (2), where $\pi_\theta(a_t|s_t)$ is policy
150 with parameter θ , q is the Q value given by policy) and plugging it into a stochastic
151 gradient ascent algorithm (Schulman et al., 2017).

$$151 \quad g = \mathbb{E}_t [\nabla_\theta \log \pi_\theta(a_t|s_t) q] \quad (2)$$

152 However, randomly changing happens during policy update of PPO1. To avoid
153 this, PPO2 imports a penalty on Kullback-Leibler (KL) divergence to the clipped
154 surrogate objective, thus it has a more stable policy updating (Schulman et al., 2017).

155 (3) Advance Actor-Critic

156 Advance Actor-Critic (A2C) combines the ingredient of both policy-based and
157 value-based to simultaneously upgrade both policy function and maximum Q value

158 (Minh et al., 2016). It uses two deep neural networks, actor-learner and critic-learner
159 to represent policy function and maximum Q value. The Actor is a reference to the
160 learned policy function, and Critic refers to the learned Q value function. The training
161 process of A2C aims to upgrade both Actor and Critic for a better control procedure.

162 2.2.3. Advantage function

163 According to above, the Q value (Eq. (1)) is mainly used as an evaluation of
164 system control. In many researches, it is replaced by the advantage function A_t (Eq.
165 (3)).

$$A_t(s_t, a_t, \theta) = q(s_t, a_t, \theta) - \max_{a_t} q(s_t, a_t, \theta) \quad (3)$$

166 The advantage function is used to measure the difference between Q value and the
167 estimation of maximum Q value (or value function), which represents ‘how much we
168 earn closer to the top’ (Minh et al., 2016). Therefore, it provides information about
169 the best control process. However, this information is estimated by sampled Q value,
170 rather than an actual maximum Q value. It may be strongly influenced by the
171 randomness of the sampling process. Thus, the advantage function can be improved
172 when a more reliable estimation is given.

173 2.3.Safety and safe reinforcement learning

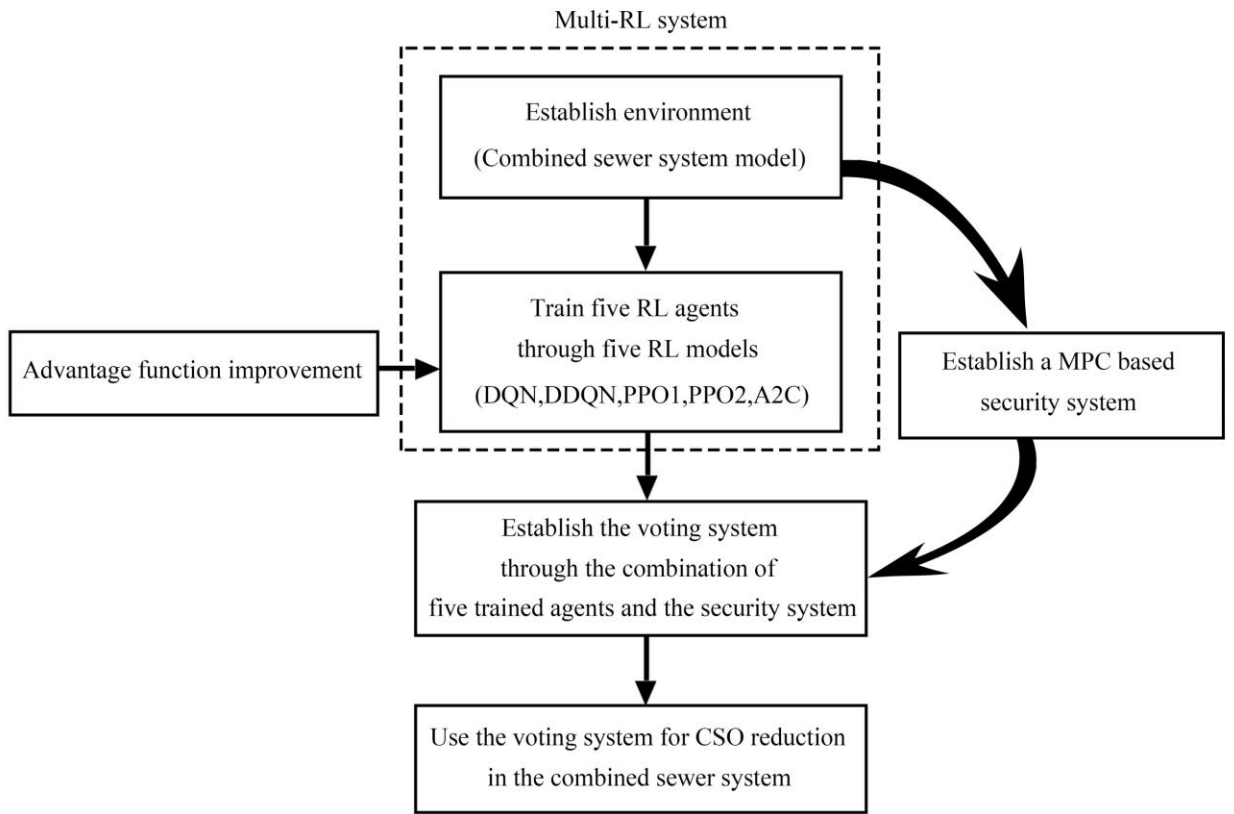
174 The safety in the RL field means to ensure reasonable system performance and
175 respect safety constraints (Garcia and Fernandez, 2015). This definition does not
176 necessarily refer to physical issues, as the detailed safety requirement is
177 problem-dependent. Usually, a stable water level of the structures and the safe
178 operation of the facilities are two reasonable safety requirements of the combined
179 sewer system.

180 In the RL literature, achieving safety usually means minimizing the variance of
181 the total expected reward (Moldovan & Abbeel, 2012), reducing the temporal
182 differences (Gehring & Precup, 2013), and avoiding the error state (Geibel and
183 Wysotzki, 2005). Two main types of methods have been developed to achieve the
184 above requirements: the optimization criterion-based method, and the exploration
185 process-based method. The first one modifies the total expected reward by taking the
186 safety as one aspect of the reward during the training process (Garcia and Fernandez,
187 2015; Castro, et al., 2012; Geibel and Wysotzki, 2005). The second one uses prior
188 knowledge to force the agent to select safe actions with higher probability in the
189 training process (Garcia and Fernandez, 2015; Yong et al., 2012; Pablo et al., 2013).

190 Although these two types of methods achieved significant improvement in the RL
191 safety, they only focus on the training process to help the agent learn to behave safely.
192 It means that both the security and control systems are coupled in one black-box
193 model. However, handing over the control process and safety check to a single
194 black-box model is not a wise choice in the real-world application, especially in civil
195 engineering (Abhiram et al., 2020). Accordingly, a security system that is independent
196 of the control system is necessary for real-world operation.

197 3. Methodology

198 A new RTC method is established through the combination of multi-RL, MPC,
199 and system optimization in this section for the improvement of safety and efficiency.
200 First, five RL agents are trained individually through five RL models with an
201 environment (a combined sewer system model). Then, a new advantage function
202 based on an optimization model is given to optimize all the RL agents for a better
203 control effect. Meanwhile, an independent MPC-based security system is designed for
204 safety check. Finally, the new RTC method is established through the combination of
205 these trained agents and the independent security system. This given RTC method is
206 used for CSO reduction in the combined sewer system. The route map is given as
207 Fig.2.



208

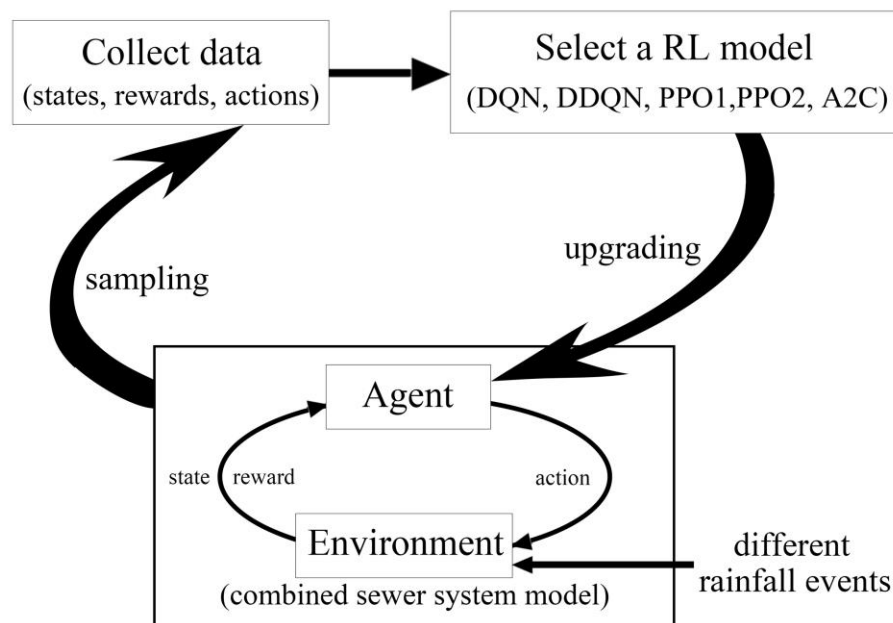
209

Fig.2 Route map

210 3.1. Multi-RLs based RTC for CSO reduction

211 We use multi-RL models to develop RTC systems for CSO reduction in the
 212 combined sewer system. Similar to previous research (Abhiram et al., 2020), the RL
 213 control systems can be described by an agent and environment. The environment
 214 represents a combined sewer system and the agent represents the entity controlling the
 215 system (Abhiram et al., 2020). During a rainfall event, an RL agent, or controller
 216 observes the state of the environment and coordinates the actions of the control assets
 217 in real-time to achieve benefits, or reward, which is the reduction of CSO in this case.
 218 The state s_t can be set as an array variable which represents useful information of
 219 sewer system at time point t . The action a_t is the control strategy of next time step
 220 given by agent with respect to the state. It can be set as a variable which indicates the
 221 operation of control assets (such as pumps, valves, gates) from time point t to time
 222 point $t + 1$. The reward r_t is a variable which represents the training target. For
 223 instance, the agent could receive positive reward for preventing CSO or a negative
 224 reward for causing CSO.

225 After establishing the agent-environment system, five RL models (including DQN,
 226 DDQN, PPO1, PPO2, and A2C) are used to train five agents separately. Although the
 227 training algorithms of each RL model are different, their basic steps are similar and
 228 can be described as follow. First, we need to collect the data of states, rewards, and
 229 actions by running the agent-environment system. It means using the agent (maybe
 230 un-trained) to control the combined sewer system model under some given rainfall
 231 events, and then collecting the state-reward-action during the process. This step is
 232 called sampling. After several rounds of sampling, the collected data is used to
 233 upgrade the agent via one of the above RL models. This step is called upgrading. The
 234 collected data contains information about the environment and our expectation of
 235 control, thus the upgrading is capable of improving the agent. The system keeps
 236 running the loop of sampling-upgrading with different rainfall events until the agent
 237 achieves a good enough control effect. Repeat these steps for five RL models, then we
 238 have five trained RL agents. This training process is shown in Fig.3.



239

240

Fig.3 Training process of multi-RL models

241

242

243

244

245

It is impossible to hand over the control of a real-world combined sewer system directly to an untrained agent. Therefore, a simulation-based scenario is strongly needed for training (Abhiram et al., 2020). We use a well-calibrated combined sewer system model (such as an SWMM model) and some rainfall events data as a prepared virtual environment.

246 3.2. Advantage function improvement

247 According to section 2.2.3, a better estimation of the maximum Q value can be
 248 achieved when we take advantage of the environment information, which is the
 249 combined sewer system in this case. Thus, we optimize the advantage function
 250 through an optimization model based on the combined sewer system to further
 251 improve the control effect of all the RL agents.

252 During sampling process, we use some given rainfall data and the combined
 253 sewer system model to find the almost best action sequence by an optimization
 254 problem. We take the objective of reducing total CSO as an example (Eq. (4)).

$$\begin{aligned} & \min \sum_{t \in \{0,1,\dots,T\}} CSO_t \\ \text{s.t.} \quad & CSO_t, s_t = \text{pipeline_model}(\text{runoff}_t, a_t, \theta) \\ & \text{runoff}_t = \text{runoff_model}(\text{rain}_t, \mu) \end{aligned} \quad (4)$$

255 Where CSO_t is the CSO volume in the time interval from t to $t + 1$, the
 256 runoff_model and pipeline_model are the models of combined sewer system
 257 with parameters θ and μ . The rain_t is the rain intensity in the time interval from t
 258 to $t + 1$, the time span has totally T time interval. The $\{a_t\}, t \in \{0,1, \dots, T\}$ is the
 259 action sequence. The $\{s_t\}, t \in \{0,1, \dots, T\}$ is the corresponding system state.

260 The optimal action $\{\hat{a}_t\}, t \in \{0,1, \dots, T\}$ and its corresponding state $\{\hat{s}_t\}, t \in$
 261 $\{0,1, \dots, T\}$ can be obtained by solving this optimization model. Any solving
 262 algorithm can be applied. In this study, a basic genetic algorithm (GA) is used to
 263 solve Eq. (4). These optimal actions and states can be used to estimate a new
 264 maximum Q value (Eq. (5)), and then generate a new advantage function (Eq. (6)).
 265 Finally, we use this new advantage function to replace the original one in each RL
 266 models (including DQN, DDQN, PPO1, PPO2, A2C). This process of the advantage
 267 function improvement (AFI) is shown in Fig.4.

$$\max_{a_t} q(s_t, a_t, \theta) \approx q(\hat{s}_t, \hat{a}_t, \theta) = \mathbb{E}_t \left[\sum_{k=0}^{\infty} [\gamma^k r_{t+k+1} | \hat{a}_t, \hat{s}_t, \theta] \right] \quad (5)$$

$$\bar{A}_t(s_t, a_t, \theta) = q(s_t, a_t, \theta) - q(\hat{s}_t, \hat{a}_t, \theta) \quad (6)$$

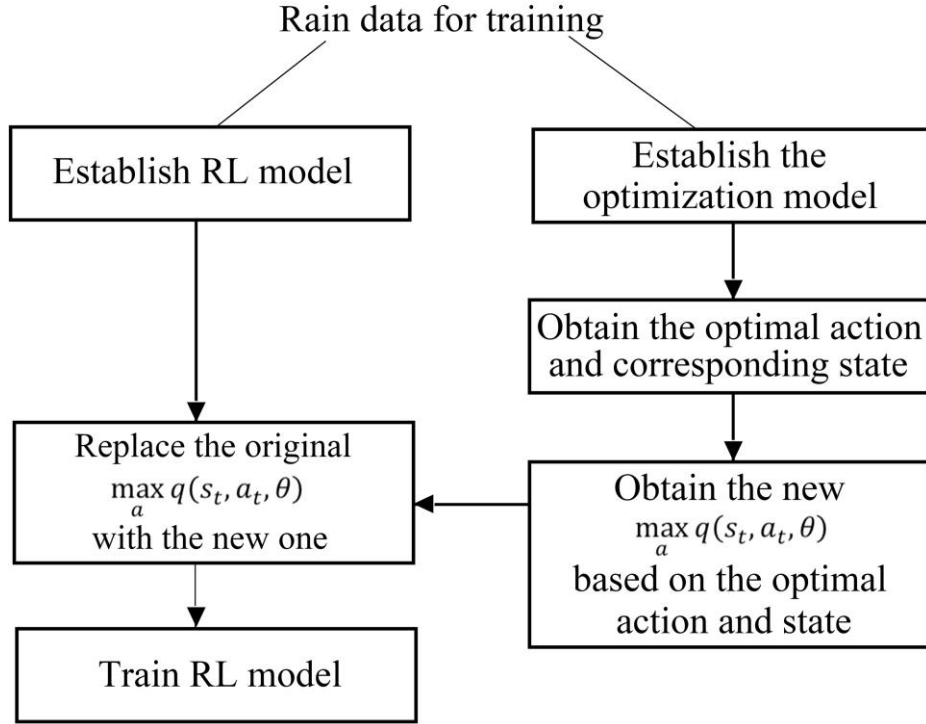


Fig.4 Advantage function improvement

These optimal actions and states give an estimation that is much closer to the maximum Q value of a given rainfall event, thus they are able to lead a better training effect. Also, the solving process of the optimization problem is decoupled from RL training, the only thing it provided is the estimation of the maximum Q value. Thus, the optimization problem can be computing on a parallel CPU.

We use the improvement rate (IR, Eq. (7)) as the indices of AFI performance. Where $CSO_{AFI,t}$ is the CSO volume of the RL models with AFI in the time interval from t to $t + 1$, $CSO_{non_AFI,t}$ is the CSO volume of RL models without AFI in the time interval from t to $t + 1$. The BL is the baseline of total COS volume, which can be provided through other RTC method or uncontrolled process. Thus, the $BL - \sum_{t \in \{0,1,\dots,T\}} CSO_{AFI,t}$ and $BL - \sum_{t \in \{0,1,\dots,T\}} CSO_{non_AFI,t}$ mean the CSO reduction of AFI model and non AFI model compared to baseline. A large IR indicates a better performance of AFI.

$$IR = \frac{(BL - \sum_{t \in \{0,1,\dots,T\}} CSO_{AFI,t}) - (BL - \sum_{t \in \{0,1,\dots,T\}} CSO_{non_AFI,t})}{(BL - \sum_{t \in \{0,1,\dots,T\}} CSO_{non_AFI,t})} \quad (7)$$

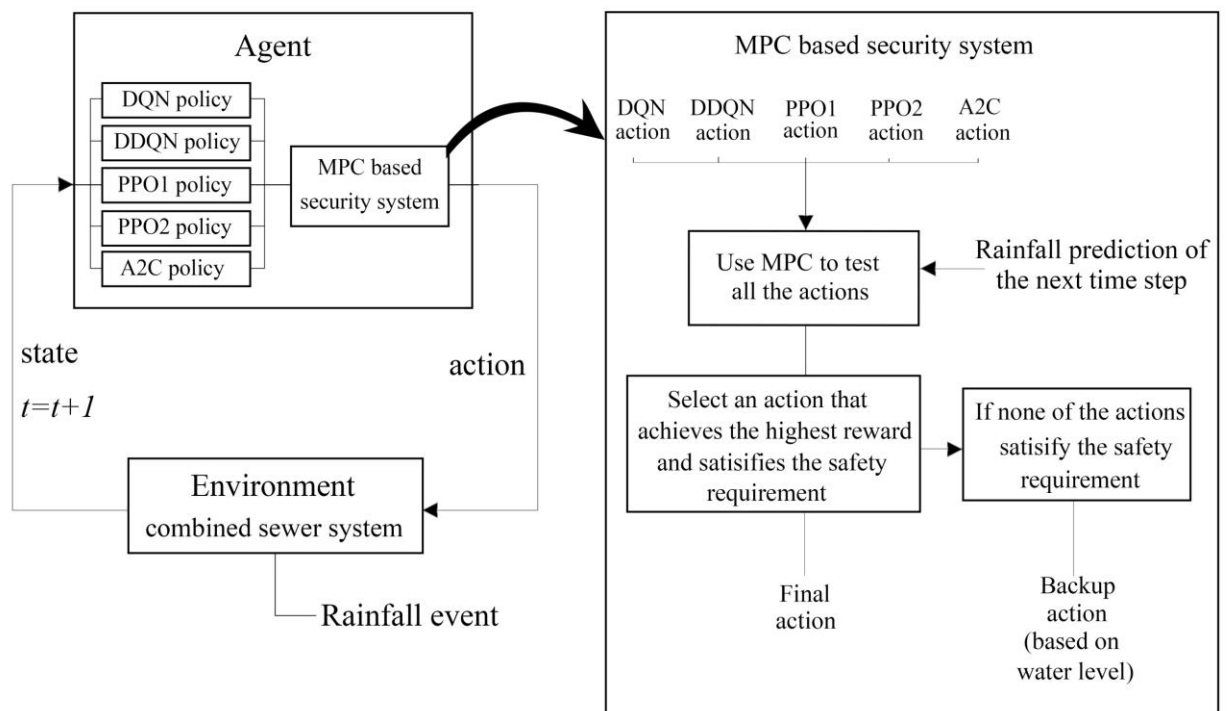
3.3. Independent security system and the voting system

After training process, these five trained agents together with an MPC based security system are used to formulate our RTC system for safe control (Fig.5). In each

286 time step, all the five trained agents give their action reference to the same state of
 287 environment. Then, the security system predicts the rainfall of the next time-step, and
 288 test all of these five actions through an MPC model. After that, the action that satisfies
 289 the safety requirement and achieves the highest reward will be chosen as the control
 290 strategy of the next time-step. For easy understanding, this combined system,
 291 including the multi-RLs and the security system, is called as voting system in the rest
 292 of the paper, as it is similar to a voting process.

293 The safety requirements in the security system are problem-dependent. For
 294 instance, some drainage systems need a low water level in some of their nodes, or a
 295 reasonable load for pumps. Therefore, the requirements should be designed
 296 individually based on the system situations. In this case, the low water level of some
 297 nodes in the pipeline network is used as the safety requirements.

298 With this one-step checking, it is possible to choose a safe action, thus provide a
 299 guarantee of safety. Also, if all the actions given by these five agents are not safe
 300 enough, the system will provide a backup choice as the output action, such as
 301 water-level based action. Because the security system is decoupled from the RL
 302 framework, it offers an objective judgment on the given actions without influence
 303 from any of the agents, thus further ensure the reliability.



304
 305

Fig.5 Security system and voting system

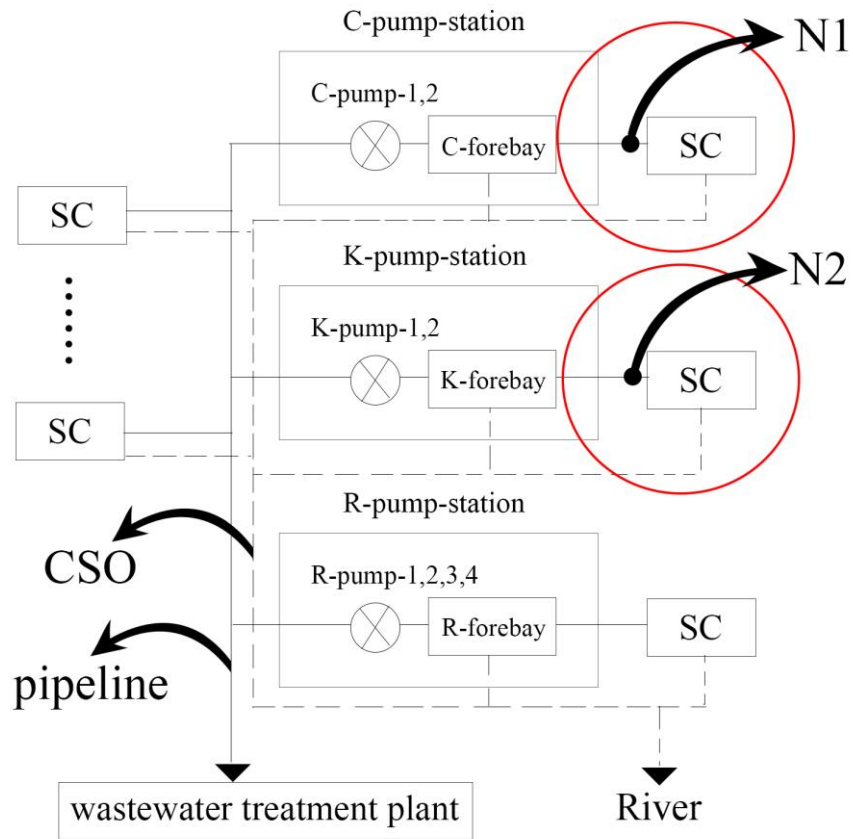
306 4. Case study

307 4.1. Combined sewer system of study area

308 The case study is the combined sewer system in a city in eastern China. It contains
309 211 nodes, 210 pipelines, and three pump stations, which includes C-pump station,
310 K-pump station and R-pump station. C-pump station and K-pump station have one
311 forebay and two pumps while the R-pump station has one forebay and four pumps.
312 Considering the risk to property and public safety, a SWMM model of this combined
313 sewer system is used as the environment. The schematic diagram of the model is
314 shown in Fig.6. More details of this model can be found in our previous researches
315 (Liao et al., 2019; Zhi et al., 2019).

316 According to Zhi et al. (2020), the areas that are vulnerable to flooding and
317 overflow in this city (called high-risk areas) are located in the sub-catchments closed
318 to the C and K pump station (red circles in Fig.6). Therefore, in this case, a reasonable
319 safety requirement of the system operation can be defined as follow: The C,
320 K-forebay, and the nodes in the high-risk sub-catchments (such as N1 and N2 in Fig.6)
321 should keep a low water level during operation.

322 Currently, this combined sewer system has its own designed RTC system, which
323 is water-level based. It sets a sequence of water-level threshold values, or set-points,
324 to operate the pumps. The pump starts working if the water level of the forebay
325 reaches its onset threshold and shuts down when the water level falls down to the
326 shutoff threshold. The detailed onset/shutoff threshold values are given in Table 1. As
327 the pumps drain water when the water level is high, this RTC system has the
328 capability of reducing CSO at some level.



329

330 Fig.6. The schematic representation of the combined sewer system model. The
 331 SCs represent the sub-catchments. The high-risk areas are highlighted by red circles
 332 (Zhi et al., 2020). The N1 and N2 are two pipeline nodes in the high-risk area.

333 Table 1. The onset/shutoff threshold values of the water level based RTC.

	Onset threshold (m)	Shutoff threshold (m)
C-pump-1	4.56	3.26
C-pump-2	4.87	4.56
K-pump-1	4.56	3.26
K-pump-2	4.87	4.56
R-pump-1	5.00	4.71
R-pump-2	6.31	5.00
R-pump-3	7.00	6.31
R-pump-4	7.78	7.00

334 4.2. Rainfall events for training

335 As numerous rainfall events are required for RL systems training, a rain pattern
 336 formula (Eq. (8)) is employed to generate rainfall events.

$$q = \frac{A(1 + C \log(P))}{|tK - i|^n} \quad (8)$$

337 Where q is the rainfall intensity, i is a designed rainfall intensity, A is the rainfall
 338 intensity with the recurrence period of one year, C is an experience parameter, P is
 339 the rainstorm return period, t is the time, K is the peak intensity position coefficient
 340 and the n is a constant. To generate enough rainfall events for RL training, these
 341 parameters are randomly chosen within a range (Table 2) based on the historical
 342 research of the rainstorm intensity formula in the study area (Wang and Xu, 2016). A
 343 total of 1,200 rainfall events were generated and used for the agent training. Each
 344 rainfall event has a four-hour duration.

345 Table 2. The range of parameters in Eq. (8)

A (mm)	C	P (year)	n	i (mm/min)	K
21~35	0.939~1.20	1~5	0.86~0.96	16~22	0.3~0.8

346

347 5. Results

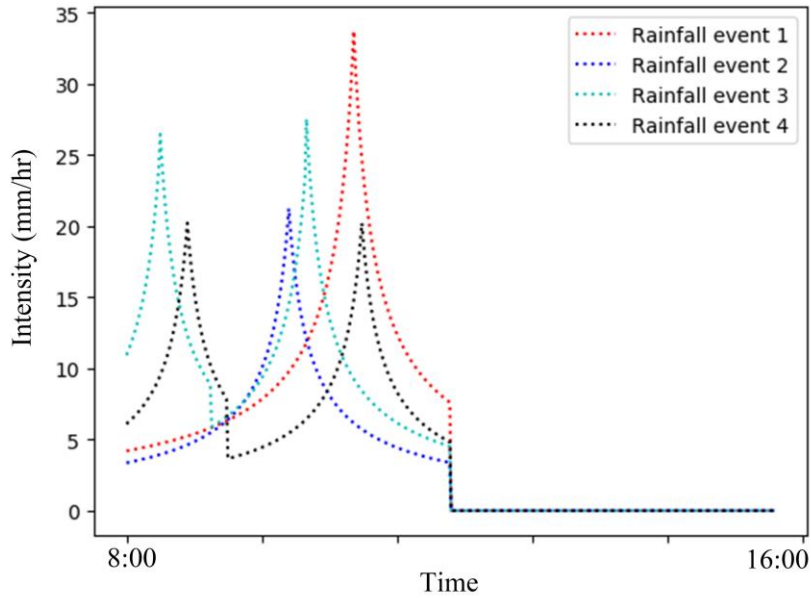
348 5.1. Configuration of the RL models

349 All the five RL models (DQN, DDQN, PPO1, PPO2, A2C) and the voting system
 350 are employed to establish RTC systems. As the control target is to reduce the total
 351 CSO during rainfall event, the state includes the current rainfall intensity, water level
 352 and water flow of forebays and volume of current total CSO. The action is an
 353 eight-dimensional vector which represents the control strategy of 8 pumps in the
 354 study area. The reward (Eq. (9)) is designed based on current CSO volume. The
 355 training process of each agent follows the steps in Section 3.1 with the rainfall data
 356 given in Section 4.2.

$$r_t = \begin{cases} -1 & \text{if CSO volume in } [t-1, t] \text{ is larger than } 0 \\ 0 & \text{else} \end{cases} \quad (9)$$

357 After training, these five agents (named as DQN, DDQN, PPO1, PPO2, A2C) and
 358 the voting system are applied for the RTC of the case study during four designed
 359 rainfall events. The rainfall intensity of these four rainfall events are given in Fig.7.
 360 Moreover, the designed rainfall events are directly used as the rainfall prediction of
 361 the voting system in all the tests to eliminate the influence of inaccuracy of rainfall
 362 predictions. Considering the risk to property and public safety, all the tests are
 363 running on the combined sewer system model mentioned above. The control interval

364 is 10 min, which means the pumps are controlled every 10 min, thus all the computing
 365 processes in one time-step, including RL agents and the MPC of the security system,
 366 should be finished within this time limit.



367

368 Fig.7 Four designed rainfall events used for the testing

369 According to the Section 4.1, the safety requirement of the voting system is
 370 defined as follow: the water level of C-forebay, K-forebay, N1, and N2 should lower
 371 than their safe line as much time as possible. The safe line of water level is set as 70%
 372 of the node depth. The depths and the safe line of each node are given in Table3. If
 373 the system is running under such a condition, we confirm that the controlling process
 374 is safe.

375 Table 3. The depth and the safe line of each node in the case study

	C-forebay	K-forebay	N1	N2
Depth (m)	5.63	5.8	2.21	1.957
Safe line (m)	3.941	4.06	1.547	1.3699

376

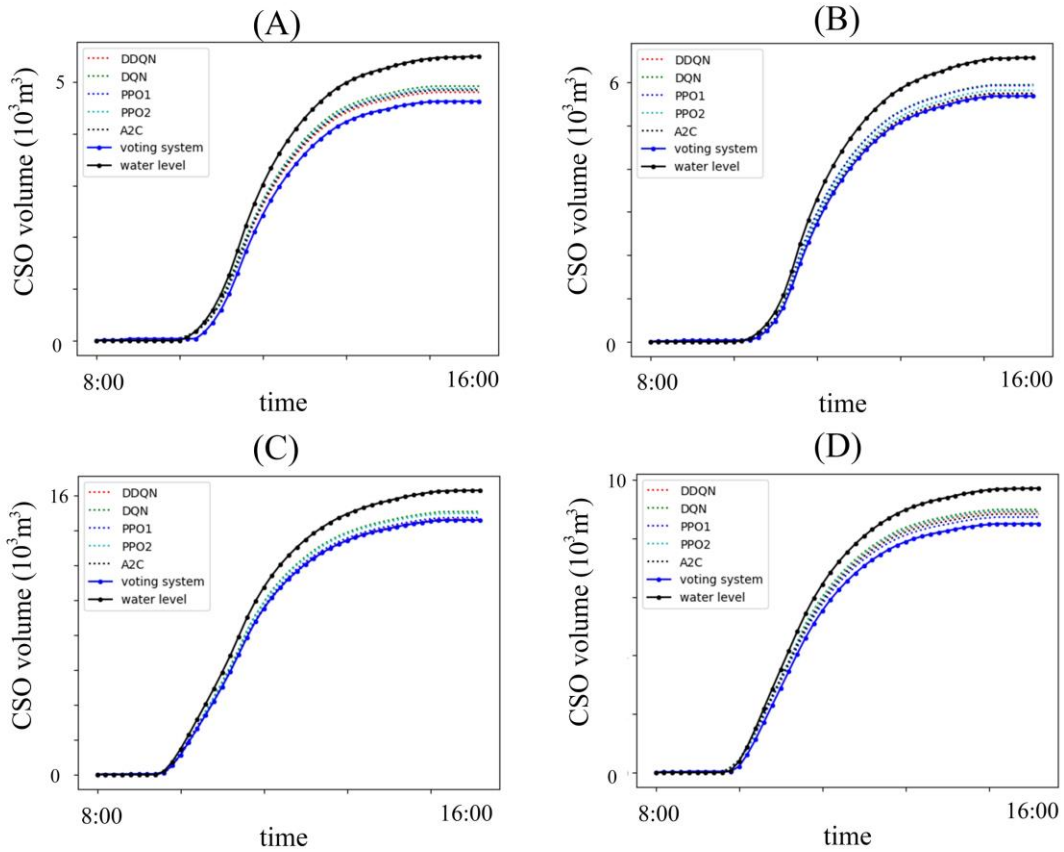
377 5.2. Efficiencies of the CSO reduction

378 The result about total overflow volume of these agents are given in Table 4. Their
 379 overflow volume at each time step during control process are given in Fig.8. For
 380 comparison, the CSO volume of the water-level based RTC system (given in Section

381 4.1) is also given. For easy understanding, we call it water level system in the rest of
 382 the paper. According to the results, all the RL models are able to show promise in
 383 CSO reduction compared to the water level system.

384 Table 4. Total overflow volume (10^3 m^3) of all the RL models during four rainfalls

	DQN	DDQN	PPO1	PPO2	A2C	Voting	Water level system
Rain1	4.926	4.807	4.876	4.878	4.847	4.631	5.503
Rain2	5.946	5.729	5.920	5.809	5.741	5.676	6.570
Rain3	15.076	14.628	14.724	14.973	14.570	14.588	16.294
Rain4	8.997	8.915	8.737	8.944	8.852	8.822	9.725



385
 386 Fig.8 Total overflow volume of all the RL models at each time point during four
 387 rainfalls.

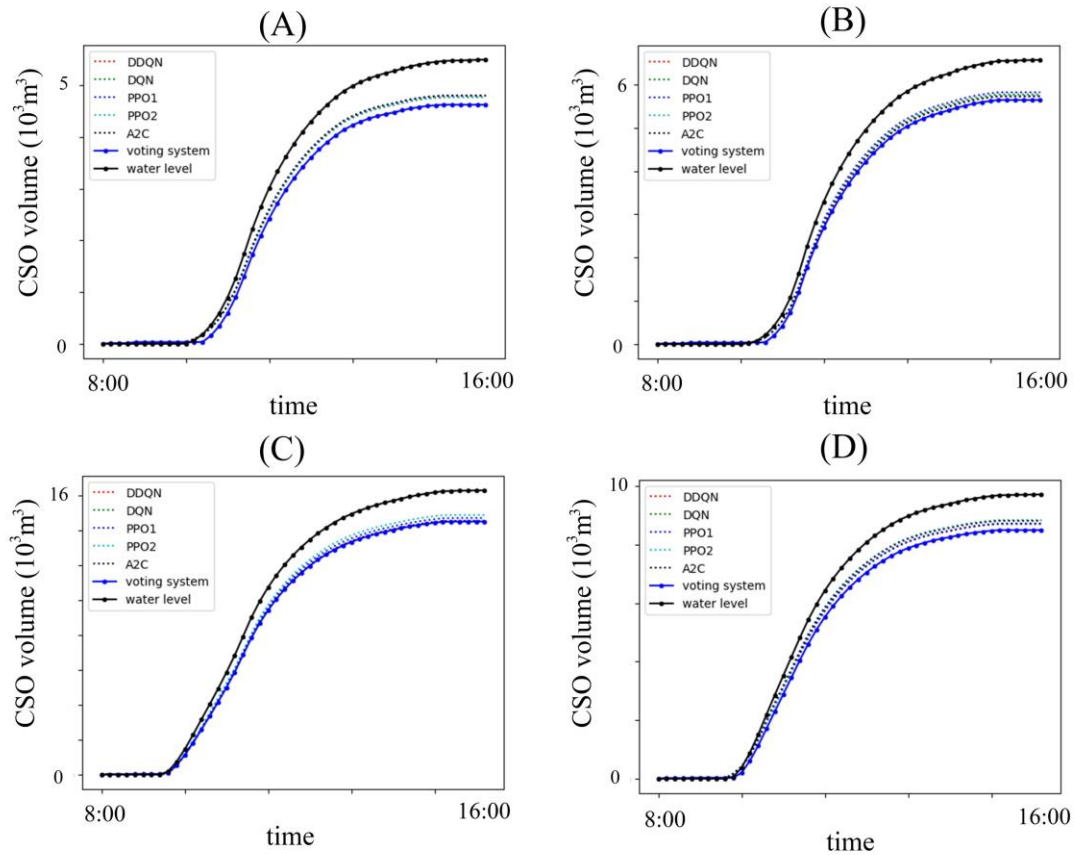
388 5.3. Advantage function improvement (AFI) on multi-RL models

389 We also employ the advantage function improvement to all the above methods for
 390 comparison. The corresponding results about total CSO volume and the improvement
 391 rate (IR, Eq. (7)) of them are given in Table 5. The baseline (BL in Eq. (7)) are
 392 provided by the CSO volume of the water level system. Their overflow volume at

393 each time step during control process are given in Fig.9. The IR is in the range from
 394 0.0% to 44.5%, which indicates that the AFI improves the CSO reduction for all the
 395 RL agents, except the DDQN in Rain2.

396 Table 5. Total CSO volume (10^3 m^3) and improvement rate (IR) of all the RL
 397 models with AFI in four rainfalls.

		Rain1	Rain2	Rain3	Rain4
DQN	CSO	4.776	5.771	14.534	8.719
	IR	26.0%	28.0%	44.5%	38.2%
DDQN	CSO	4.776	5.729	14.531	8.717
	IR	4.5%	0.0%	5.8%	24.4%
PPO1	CSO	4.805	5.82	14.707	8.73
	IR	11.3%	15.4%	1.2%	0.7%
PPO2	CSO	4.778	5.741	14.881	8.839
	IR	16.0%	8.9%	7.0%	13.4%
A2C	CSO	4.806	5.727	14.547	8.505
	IR	6.3%	1.7%	1.3%	39.7%
Voting	CSO	4.629	5.642	14.505	8.508
	IR	0.2%	3.8%	4.9%	34.8%



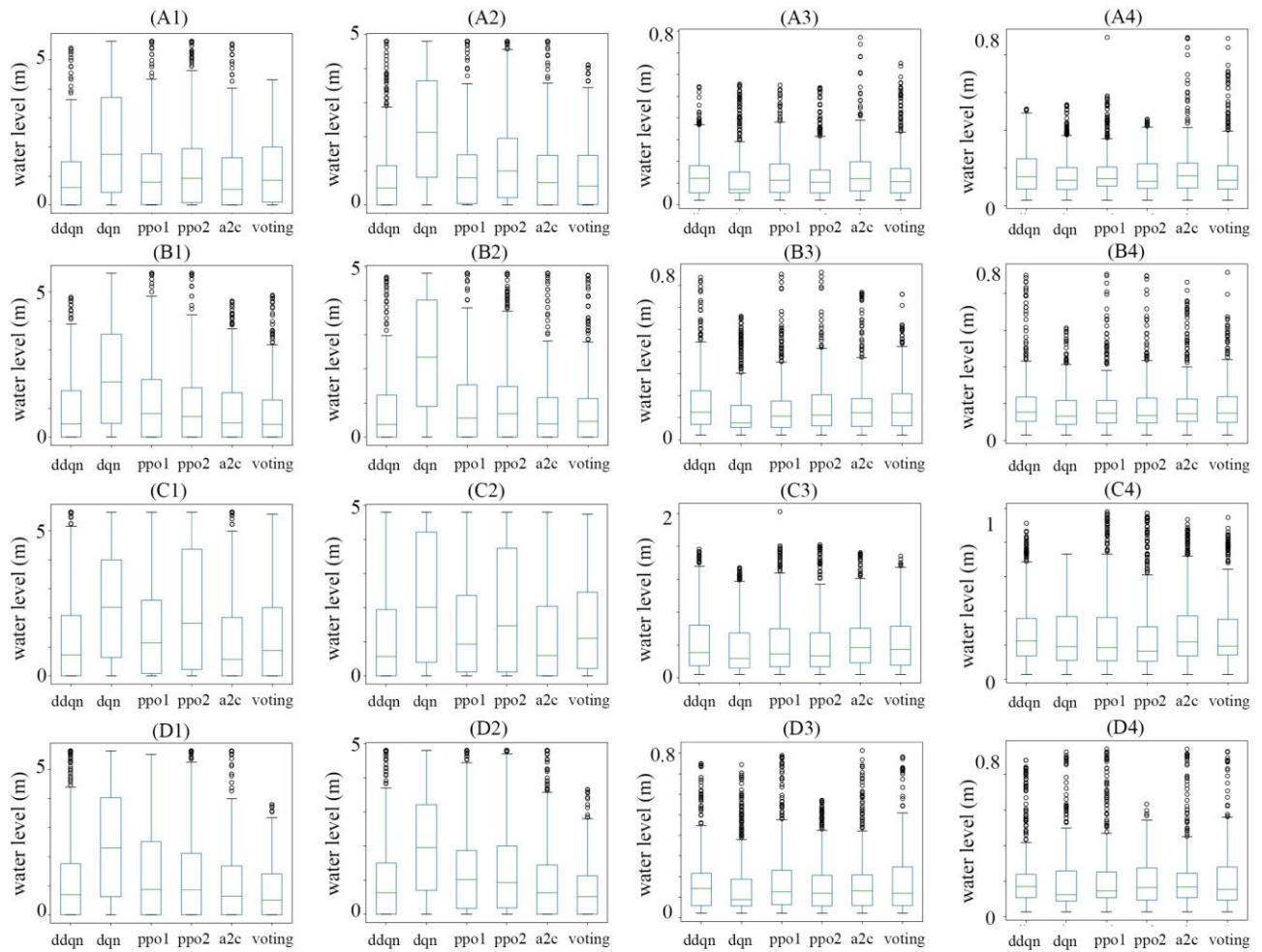
399

400 Fig.9 Total overflow volume of all the RL models (with AFI) at each time point
 401 during four rainfalls.

402 5.4. Safety of the voting system

403 To prove the safety of the voting system, the water level results of C forebay, K
 404 forebay, N1, and N2 during the rainfall duration of all the tests are given. If the water
 405 level of each node is lower than its safe line as much time as possible, then we
 406 confirm that the controlling process is safe. For each method, there are total of 480
 407 water level data points for each node (C forebay, K forebay, N1, and N2) during an
 408 eight hours rainfall event (from 8:00 to 16:00). All of these data are presented through
 409 box plot in Fig.10 (the tests without AFI) and 11 (the tests with AFI).

410 Accordingly, the water level of DQN and PPO2 in the C forebay and K forebay
 411 surpass the safe line in Table 3 (3.941 m and 4.06 m), which means that the control
 412 process given by these two methods maybe unsafe for practically application. The
 413 water level of the voting system may not be the lowest all the time, it is more likely to
 414 stay at a low rank and satisfy the safety requirements in Table 3.

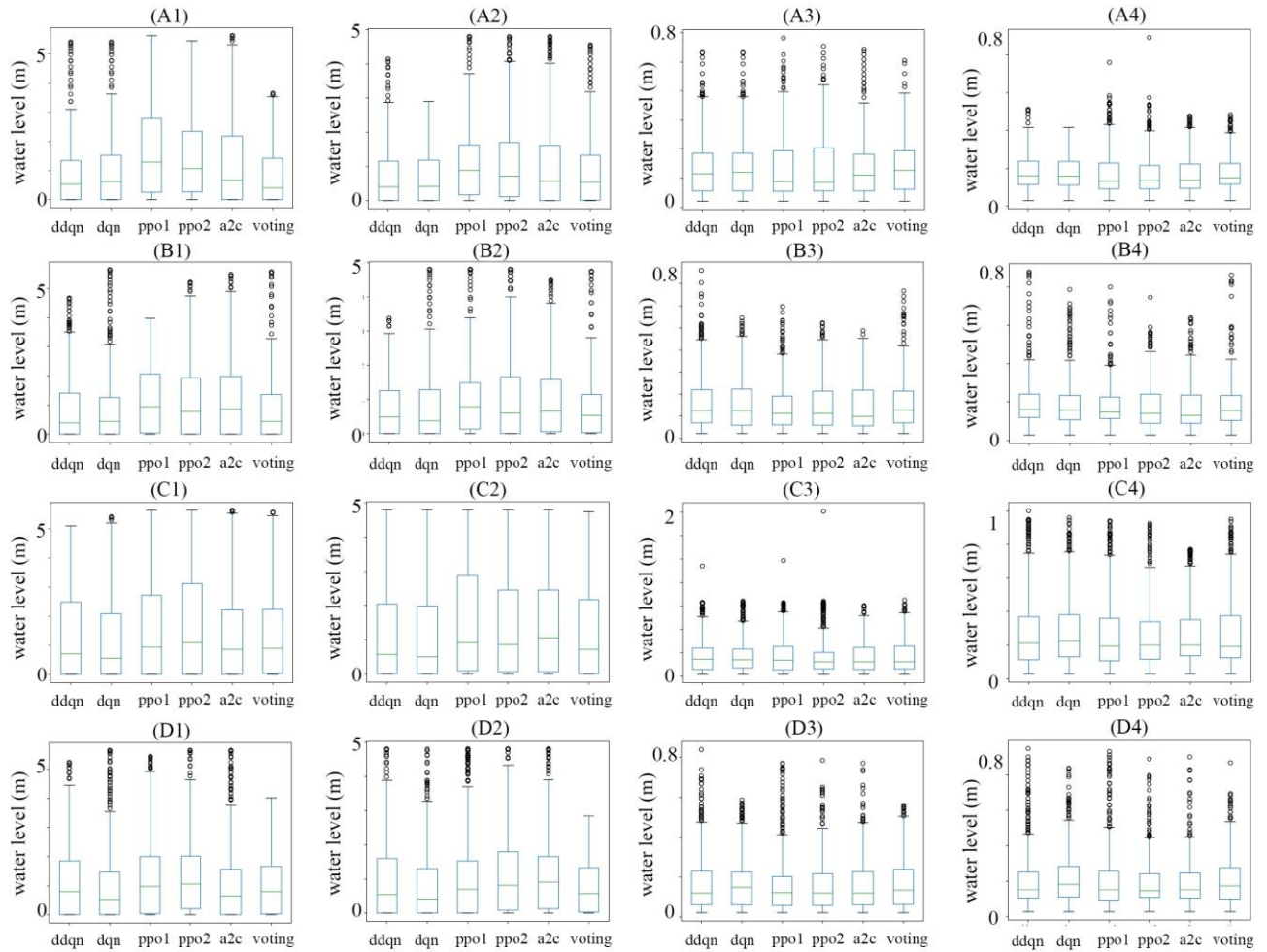


415

416 Fig.10 The water level of the C-forebay (1), K-forebay (2), N1 (3), and N2 (number 4)

417

during Rain1 (A), Rain2 (B), Rain3 (C), and Rain4 (D). Without AFI.



418
 419 Fig.11 The water level of the C-forebay (1), K-forebay (2), N1 (3), and N2 (4) during
 420 Rain1 (A), Rain2 (B), Rain3 (C), and Rain4 (D). With AFI.

421 5.5. Computational cost

422 All the trainings and testing were run on a Windows Server (Intel ® Xeon® Gold
 423 5117 CPU @2.00 GHz, RAM 32.0 GB). The training process of a single RL model
 424 took approximately 2-3 hours (with AFI) and 1-2 hour (without AFI). After training,
 425 each RL agent only needs around 0.01 s to generate action. The computing process of
 426 the security system at each time step took around 3 min, which is less than the 10 min
 427 used as control interval.

428 6. Discussion

429 6.1. CSO reduction and system optimization

430 6.1.1. The AFI efficiency and the limitation of CSO reduction

431 From the above results, all the RL models reduce the overflow, which indicates
 432 that different types of RL models, policy-based or value-based, are effective in the

433 CSO control of the combined sewer systems. Also, the AFI achieves improvement of
434 CSO reduction with the IR in the range from 0.0% to 44.5%, thus shows its efficient
435 performance.

436 Meanwhile, according to Fig.8 and Fig.9, the difference among the RL agents in
437 terms of CSO volume is getting smaller after the AFI technique is employed. The
438 reason is that the AFI helps the RL agents reach the limits of CSO reduction. In fact,
439 if the entire rainfall event can be accurately predicted and the optimization method is
440 used to search for the optimal control strategy sequence, the obtained control strategy
441 should be the global optimal solution and represents the limits of CSO reduction.
442 From this perspective, the introduction of AFI is to provide information about the
443 optimal solution may appear during the control process. Therefore, AFI helps all the
444 RL systems improve their control effect, in other words, helps them to get closer to
445 the limits of CSO reduction, which then leads to less difference among them.

446 6.1.2. Local optimization

447 The "optimal solution may appear" here indicates the local optimal solution which
448 is close to, rather than equal to, the limitation of CSO reduction. In practical RTC
449 applications, we can neither accurately predict rainfall nor solve a complex
450 optimization problem under the time constraints. Indeed, some researches sacrifice
451 the accuracy to achieve a faster simulation (Xu et al., 2013; Lund et al., 2020). It
452 means that if we want to plug the AFI into an online training process, it may lead to a
453 local optimal control strategy, rather than the global optimal one. Therefore, the AFI
454 can only be considered under off-line condition. How to ensure better optimality of
455 AFI needs to be further explored and studied in the future.

456 6.1.3. Optimization of voting system

457 According to the results, the voting system considers the optimal control strategy
458 in each step of decision making, thus lead to a relatively better performance in the
459 above examples. However, it is not necessarily optimal. For instance, in the Rain4 of
460 the second test, the control effect of the voting system is relatively poor compared to
461 A2C. The main reason is that the voting system can only guarantee the optimal of the
462 selected action in each time step, rather than the optimization of the whole control
463 process, as the optimal choice in each step may not definitely lead to the optimal of
464 final results.

465 6.2. The safety of the voting system

466 Since the control process depends on the agent, which is a black-box model, its
467 output is essentially probability-oriented and lacks the interpretability. Due to this, the
468 safety of the RLC application is naturally questioned. For instance, based on the (C1)
469 and (C2) of Fig.10, it may cause an unsafe situation if we only use DQN agent and
470 PPO2 agent, as their water level is likely to stay at a high rank. In fact, both of these
471 methods do not meet the safety requirement (given in Table 3) very well.

472 Compared to these RL models, the voting system is more likely to stay at a lower
473 water level and satisfies the safety requirements in Table 3 as much time as possible.
474 The main reason is that the voting system is able to avoid the risk caused by any one
475 of the agents by selecting a safe action from all the given choices, therefore, it is safer
476 than any single RL system during application. Although the causality between the
477 control strategy and the system state cannot be explained in principle, the voting
478 system provides a guarantee of safe operation to the control system.

479 6.3.Challenges

480 Although the computing time of each RL agent is very short (0.01 s), their
481 training process is computationally expensive, especially after adding the AFI, as each
482 step of training needs to solve an optimization problem synchronously. At present, the
483 method to speed up the training process requires the use of more powerful computing
484 equipment and parallel computing technology. According to the calculation process,
485 the consumption of computing power mainly depends on two steps: environment
486 simulation (SWMM model in this article) and RL training. How to optimize the
487 calculation speed from these two aspects is what we are considering.

488 In addition, it needs to explain that the control strategy provided by RL agents
489 only aims to minimize the overflow under the premise of a given rainfall event and a
490 combined sewer system. If the entire sewer system is overloaded, simply relying on
491 the RL control to adjust the hydrodynamics of the pipeline network cannot
492 fundamentally reduce the overflow. This is one of the drawbacks faced by all the RTC
493 methods.

494 7. Conclusion

495 Considering the safety and control effect improvement, a new RTC method based
496 on multi-reinforcement learning, MPC, and an optimization model is introduced in
497 this study. First, five individual agents are trained individually via five RL models.
498 Then, an optimization model is applied to improve the advantage function of all the

499 RL agents. After that, an independent MPC based security system is established to
500 ensure the safety of control strategy. Finally, our RTC method is established through
501 the combination of these five agents and the independent security system.

502 The methodology and the case study show that: (i) Different RL methods are able
503 to show promise in CSO reduction. (ii) The AFI technique imports the information of
504 the optimal control strategy given by a corresponding optimization model, thus
505 provide an improvement of CSO reduction with the maximum improvement rate of
506 44.5%. (iii) The security system is able to select a relatively better control strategy (or
507 action) among all the actions given by agents and check its safety before use it. (iv)
508 The voting system may lead to a relatively better control effect, but it is not
509 necessarily optimal, because the optimal choice in each step may not definitely lead to
510 the optimal of final results.

511 Meanwhile, our method is not a perfect solution. The AFI is suffered from the
512 problem of local optimization. The training process of all the RL models are
513 computationally expensive. Moreover, the control effect of RL control may be limited
514 when the combined sewer system is overloaded, as it only provides a solution under
515 the premise of a given rainfall event rather than extends the capacity of combined
516 sewer system.

517

518 Acknowledgements

519 This study was financially supported by the Major Science and Technology
520 Program for Water Pollution Control and Treatment (grant no. 2018ZX07208006) and
521 the National Natural Science Foundation of China (grant no. 51778451). We also
522 thank the 111 Project (B13017) of Tongji University.

523 Data for this research, which is the calibrated SWMM model in the case study, is
524 available in these references: Liao et al., (2019) and Zhi et al., (2019).

525

526 Reference

527 Abhiram Mullanpudi, Matthew J. Lewis, Cyndee L. Gruden, Branko Kerkez. (2020).

528 Deep reinforcement learning for the real time control of stormwater
529 systems, *Advances in Water Resources*, Volume 140.

530 Castelletti A, Pianosi F, Restelli M. (2013). A multiobjective reinforcement learning
531 approach to water resources systems operation: Pareto frontier

532 approximation in a single run. *Water Resources Research*, 49(6): 3,476–
533 3,486.

534 Castro, D. D., Tamar, A., & Mannor, S. (2012). Policy Gradients with Variance
535 Related Risk Criteria. international conference on machine learning.

536 Congcong S., Luis R., Bernat J., Jordi M., Eduard M., Ramon G., Montse M., Vicenç
537 P., Gabriela C. (2020). Integrated pollution-based real-time control of
538 sanitation systems. *Journal of Environmental Management*. Volume 269,
539 2020, 110798, ISSN 0301-4797

540 Fu G, Butler D, Khu S T. (2008). Multiple objective optimal control of integrated
541 urban wastewater systems. *Environmental Modelling & Software*, 2008,
542 23(2): 225-234.

543 Garcia, J., & Fernandez, F. (2015). A comprehensive survey on safe reinforcement.
544 learning. *Journal of Machine Learning Research*, 16(1), 1437-1480.

545 Geibel, P., & Wyszotzki, F. (2005). Risk-sensitive reinforcement learning applied to
546 control under constraints. *Journal of Artificial Intelligence Research*,
547 24(1), 81-108.

548 Gehring, C., & Precup, D. (2013). Smart exploration in reinforcement learning using
549 absolute temporal difference errors. *adaptive agents and multi agents*
550 *systems*.

551 Gu X, Liao Z, Zhang G, et al. (2017). Modelling the effects of water diversion and
552 combined sewer. overflow on urban inland river quality. *Environmental*
553 *Science and Pollution Research*, 2017, 24(26): 21038-21049.

554 Joseph-Duran B, Ocampo-Martinez C, Cembrano G. (2015). Output-feedback control
555 of combined sewer networks through receding horizon control with
556 moving horizon estimation. *Water Resources Research*, 51(10):
557 8,129-8,145.

558 Kerkez, B., Gruden, C., Lewis, M.J., Montestruque, L., Quigley, M., Wong, B.P.,
559 Bedig, A., Kertesz, R., Braun, T., Cadwalader, O., Poresky, A., Pak, C.
560 (2016). Smarter Stormwater Systems. *Environ. Sci. Technol.* 50 (14).

561 Labadie J W. (2014). *Advances in Water Resources Systems Engineering:*
562 *Applications of Machine Learning*. *Modern Water Resources*
563 *Engineering*. Humana Press, Totowa, NJ: 467–523.

564 Liao, Z., Gu, X., Xie, J. et al. (2019). An integrated assessment of drainage system
565 reconstruction based on a drainage network model. *Environ Sci Pollut*
566 *Res* 26: 26563.

567 Lund N S V, Falk A K V, Borup M, et al. (2018). Model predictive control of urban
568 drainage systems: A review and perspective towards smart real-time water
569 management. *Critical reviews in environmental science and technology*,
570 2018, 48(3): 279-339.

571 Lund, N. S. V., Borup, M., Madsen, H., Mark, O., & Mikkelsen, P. S. (2020). CSO
572 reduction by integrated model predictive control of stormwater inflows: A
573 simulated proof of concept using linear surrogate models. *Water Resources*
574 *Research*, 56, e2019WR026272.

575 Madani K, Hooshyar M. (2014). A game theory–reinforcement learning (GT–RL)
576 method to develop optimal operation policies for multi-operator reservoir
577 systems. *Journal of hydrology*, 519: 732–742.

578 Mailhot A., Talbot G., Lavallée, B. (2015). Relationships between rainfall and
579 Combined Sewer Overflow (CSO) occurrences. *Journal of Hydrology*,
580 2015, 523:602-609.

581 Minh, V., Kavukcuoglu, K., Silver, D., Rusu, A.a., Veness, J., Bellemare, M.G.,
582 Graves, A., Riedmiller, M., Fidjeland, A.K., Ostrovski, G., Petersen, S.,
583 Beattie, C., Sadik, A., Antonoglou, I., King, H., Kumaran, D., Wierstra,
584 D., Legg, S., Hassabis, D. (2015). Human-level control through deep
585 reinforcement learning. *Nature* 518, 529–533.

586 Minh, V., Badia, A. P., Mirza, M., Graves, A., Harley, T., Lillicrap, T., Silver, D.,
587 Kavukcuoglu, K. (2016). Asynchronous methods for deep reinforcement
588 learning. *international conference on machine learning*.

589 Moldovan, T., & Abbeel, P. (2012). Safe Exploration in Markov Decision
590 Processes. *arXiv: Learning*.

591 Ochoa, D., Rianobriceno, G., Quijano, N., & Ocampomartinez, C. (2019). Control of
592 Urban Drainage Systems: Optimal Flow Control and Deep Learning in
593 Action. *advances in computing and communications*.

594 Pablo Quintia Vidal, Roberto Iglesias Rodriguez, Miguel Rodriguez Gonzalez, and
595 Carlos V azquez Regueiro. (2013). Learning on real robots from

596 experience and simple user feedback. *Journal of Physical Agents*, 7(1),
597 ISSN 1888-0258.

598 Pan, X., You, Y., Wang, Z., & Lu, C. (2017). Virtual to real reinforcement learning
599 for autonomous driving. arXiv preprint arXiv:1704.03952.

600 Rauch W, Harremoes P. (1999). Genetic algorithms in real time control applied to
601 minimize transient pollution from urban wastewater systems. *Water*
602 *research*, 1999, 33(5): 1265-1277.

603 Schütze M, Campisano A, Colas H, et al. (2002). Real-time control of urban
604 wastewater systems-where do we stand today? *Global Solutions for Urban*
605 *Drainage*. 2002: 1-17.

606 Schulman, J., Wolski, F., Dhariwal, P., Radford, A., & Klimov, O. (2017). Proximal
607 Policy Optimization Algorithms. arXiv: Learning.

608 Schulman, J., Levine, S., Abbeel, P., Jordan, M. I., & Moritz, P. (2015). Trust Region
609 Policy Optimization. international conference on machine learning.

610 Sebastian Peitz, Stefan Klus. (2019). Koopman operator-based model reduction for
611 switched-system control of PDEs. *Automatica*. 106, 184-191.

612 Shao K, Zhu Y, Zhao D. (2018). StarCraft Micromanagement with Reinforcement
613 Learning and Curriculum Transfer Learning. *IEEE Transactions on*
614 *Emerging Topics in Computational Intelligence*.

615 Silver, D., Schrittwieser, J., Simonyan, K., Antonoglou, I., Huang, A., Guez, A., &
616 Chen, Y. (2017). Mastering the game of go without human knowledge.
617 *Nature*, 550(7676), 354.

618 Suarez J, Puertas J. (2005). Determination of COD, BOD, and suspended solids loads
619 during combined sewer overflow (CSO) events in some combined
620 catchments in Spain. *Ecological Engineering*, 24(3): 199–217.

621 Sutton R S, Barto A G. (2018). Reinforcement learning: An introduction[M]. MIT
622 press.

623 Sutton, R. S., Mcallester, D., Singh, S., & Mansour, Y. (1999). Policy Gradient
624 Methods for Reinforcement Learning with Function Approximation.
625 *neural information processing systems*.

626 Tan Zhiyong, Chai Quek, Philip Y.K. Cheng. (2001). Stock trading with cycles: A
627 financial application of ANFIS and reinforcement learning. *Expert*
628 *Systems with Applications*, 38(5):4741-4755.

629 Van Hasselt, H., Guez, A., & Silver, D. (2016). Deep reinforcement learning with
630 double Q-Learning. *national conference on artificial intelligence*.

631 Van Hasselt. (2010). Double Q-learning. *Advances in Neural Information Processing*
632 *Systems*, 23:2613–2621.

633 Wang, Z., Schaul, T., Hessel, M., Van Hasselt, H., Lanctot, M., & De Freitas, N.
634 (2016). Dueling network architectures for deep reinforcement learning.
635 *international conference on machine learning*.

636 Wan P, Lemmon M D. (2007). Distributed flow control using embedded
637 sensor-actuator networks for the reduction of combined sewer overflow
638 (CSO) events. 2007 46th IEEE Conference on Decision and Control.
639 IEEE: 1,529–1,534.

640 Wang Rui, Xu Deqian. (2016). Derivation of Rainstorm Intensity Formula for Hefei
641 City. *Journal of China Hydrology*, 2016, 36(1): 71-74.

642 Wu, B. (2019). Hierarchical macro strategy model for moba game ai. In *Proceedings*
643 *of the AAAI Conference on Artificial Intelligence*. Vol. 33, pp.
644 1206-1213.

645 Xie J, Chen H, Liao Z, et al. (2017). An integrated assessment of urban flooding
646 mitigation strategies for robust decision making. *Environmental*
647 *modelling & software*, 2017, 95: 143-155.

648 Xu Z, Liao Z. (2013). A Systematic View Is Key: The Successful Case of Suzhou
649 Creek Rehabilitation. *Environmental Science & Technology*, 47(21):
650 11,936–11,937.

651 Xu, M., Van Overloop, P. J., & De Giesen, N. C. (2013). Model reduction in model
652 predictive control of combined water quantity and quality in open
653 channels. *Environmental Modelling and Software*, 72-87.

654 Yong Song, Yi bin Li, Cai hong Li, and Gui fang Zhang. (2012). An efficient
655 initialization approach of q-learning for mobile robots. *International*
656 *Journal of Control, Automation and Systems*, 10(1):166–172.

657 Zhi Guozheng, Liao Zhenliang, Wenchong Tian, Jiang Wu. (2020). Urban flood risk
658 assessment and analysis with a 3D visualization method coupling the
659 PP-PSO algorithm and building data. *Journal of Environmental*
660 *Management*. Volume 268, 110521, ISSN 0301-4797.

661 Zhi G, Liao Z, Tian W, Jiang W. (2019). A 3D dynamic visualization method coupled
662 with an urban drainage model. *Journal of Hydrology*, 577: 123988.